minerals

MDPI

Article

Supported Hybrid Amines Within Porous Aluminosilicate Clays with Natural Different Morphologies for Efficient CO_2 Capture

Xiaoyu Li [1], Jie Chen [1], Wenqing Zhang [1], Chenyu Wang [1], Hui Ma [1], Kang Peng [2,*] and Zheng Zhou [3,*]

[1] School of Materials Science and Engineering, Chang'an University, Xi'an 710064, China; leexy@chd.edu.cn (X.L.)
[2] State Key Laboratory for Mechanical Behavior of Materials, Xi'an Jiaotong University, Xi'an 710049, China
[3] State Grid Zhejiang Electric Power Research Institute, Hangzhou 310014, China
* Correspondence: pengkangtm@xjtu.edu.cn (K.P.); zhouzheng1020@zju.edu.cn (Z.Z.)

Abstract: The urgent need for efficient CO_2 capture technologies has driven research into amine-functionalized adsorbents, though existing methods face trade-offs between adsorption capacity and cycling stability. This study addresses these limitations by developing a novel hybrid modification strategy combining chemical grafting and physical impregnation on polymorphic kaolinite minerals. Through systematic acid leaching and hybrid grafting–impregnation amine functionalization, the adsorbents with hierarchically porous structures and optimized performances are synthesized. The tubular adsorbent (ATK-APTES-PEI) demonstrated exceptional performance, achieving a CO_2 uptake of 1.68 mmol/g at 75 °C under a 60% CO_2/40% N_2 mixed gas flow, with only 5.3% capacity loss after 10 adsorption–desorption cycles, significantly outperforming both rod-like (ARK-APTES-PEI, 1.55 mmol/g) and flake-like (AFK-APTES-PEI, 1.23 mmol/g) variants. The unique pore structure of ATK-APTES-PEI enables simultaneous high amine loading and maintained gas diffusion pathways, while the hybrid modification strategy synergistically enhances both adsorption capacity and stability by increasing active surface sites. These findings establish critical structure–property relationships for mineral-based adsorbents and demonstrate a scalable approach for industrial CO_2 capture applications. The work provides a blueprint for designing cost-effective, stable adsorbents using abundant clay minerals, bridging materials science with environmental engineering for sustainable carbon management solutions.

Keywords: kaolin; morphology; supported hybrid amines; CO_2 adsorption

check for updates

Academic Editor: Rafael Santos

Received: 30 March 2025
Revised: 3 May 2025
Accepted: 8 May 2025
Published: 9 May 2025

Citation: Li, X.; Chen, J.; Zhang, W.; Wang, C.; Ma, H.; Peng, K.; Zhou, Z. Supported Hybrid Amines Within Porous Aluminosilicate Clays with Natural Different Morphologies for Efficient CO_2 Capture. *Minerals* **2025**, *15*, 506. https://doi.org/10.3390/min15050506

Copyright: © 2025 by the authors. Licensee MDPI, Basel, Switzerland. This article is an open access article distributed under the terms and conditions of the Creative Commons Attribution (CC BY) license (https://creativecommons.org/licenses/by/4.0/).

1. Introduction

The problem of the environment and development is the focus of universal concern in the world today. The greenhouse effect caused by the emission of greenhouse gases into the atmosphere and the negative impact on human beings and the natural environment have attracted wide attention from governments all over the world [1–3]. As the most consequential greenhouse gas, carbon dioxide (CO_2) has exhibited a persistent increase in global concentration since the Industrial Revolution [4]. This upward trajectory in CO_2 levels inevitably contributes to global climate warming, posing substantial threats to human survival and development. In response, nations across the world have implemented diverse measures to mitigate carbon emissions and alleviate environmental pressures stemming from greenhouse effects, with carbon capture and storage (CCS) technologies receiving particular focus [5,6].

Among existing CO_2 capture technologies, liquid amine absorption methods face limitations in broader applications due to several inherent drawbacks: equipment corrosion, solvent volatility, high energy requirements for regeneration, poor cycling performance, and limited effectiveness for low-to-medium concentration CO_2 streams [7]. In contrast, amine-functionalized adsorbents prepared by immobilizing liquid amines onto solid substrates combine the advantages of liquid amines while overcoming their limitations. Consequently, CO_2 capture using amine-functionalized solid adsorbents has emerged as a highly promising technology, stimulating extensive research efforts. Therefore, it is urgent to develop efficient and cost-effective CO_2 solid adsorbents.

Common solid adsorbent supports include activated carbon [8], mesoporous silica materials [9–11], zeolite molecular sieve [12], organic polymers [13], metal–organic frameworks (MOFs) [14,15], alkali metal carbonates [16,17] and natural porous clay minerals [18,19]. Among these, natural clay minerals stand out due to their abundant availability, low cost, favorable pore structures, chemical tunability, and structural stability, making them excellent matrix materials. However, unmodified clay minerals exhibit limited CO_2 adsorption capacity, necessitating amine functionalization to enhance performance. Kaolinite, a representative clay mineral, exhibits limited CO_2 adsorption capacity in its unmodified state due to surface chemical inertness, restricted pore structures, and moisture sensitivity. To enhance CO_2 adsorption performance, amine functionalization is required to introduce chemisorption sites, optimize pore architectures and improve stability, as demonstrated by the hybrid grafting–impregnation strategy in this study [20–23]. Currently, two primary amine functionalization methods exist.

Physical impregnation: This method involves dissolving liquid amines in alcoholic solutions, loading them into porous materials through impregnation, followed by solvent evaporation to yield amine-functionalized CO_2 adsorbents [24]. Wang et al. utilized montmorillonite nanosheets as a support to load polyethyleneimine (PEI) via the solution impregnation method, investigating its CO_2 adsorption behavior. The results indicated that the material exhibited a significantly lower cost compared to conventional adsorbents while achieving enhanced CO_2 adsorption performance [18]. PEI was impregnated onto silica nanoflowers by Kole et al., achieving a CO_2 adsorption capacity of 1.27 mmol/g under pure CO_2 at 25 °C, which demonstrates suitability for carbon management in confined spaces [25]. While this approach achieves high CO_2 adsorption capacity, the resulting materials typically demonstrate poor cycling stability and short service lives [18,19]. Chemical grafting: This technique covalently bonds amine molecules to surface hydroxyl groups of the matrix material through chemical reactions. 3-aminopropyltriethoxysilane (APTES)-functionalized hollow silica microspheres developed by De et al. demonstrated efficient CO_2 adsorption at relatively low temperatures, making them suitable for confined spaces such as submarines and spacecraft cabins [26]. Jana et al. grafted APTES on halloysite nanotubes outer surface, enabling reversible CO_2 adsorption from air with fractional-order adsorption kinetics [27]. Although chemically grafted adsorbents exhibit superior chemical stability and recyclability, their CO_2 adsorption capacity tends to be lower [27–29]. By combining the strengths of both functionalization approaches through a hybrid physical impregnation–chemical grafting strategy, several advantages can be realized: improved amine loading efficiency, increased active surface sites, enhanced interfacial forces, promoted CO_2 diffusion within pore structures, and reduced toxicity and corrosivity associated with liquid organic amines [30–33].

This study builds upon existing CO_2 capture methodologies by employing kaolinite minerals as matrix materials. Through a novel surface modification technique integrating both the chemical grafting of APTES and physical impregnation of PEI, this study aims to significantly enhance CO_2 adsorption performances of kaolins, ultimately developing

a cost-effective, efficient, and stable kaolinite-based CO_2 solid adsorbent. The innovative aspect of this study lies in the systematic investigation of the effects of natural characteristics of kaolinite, including morphology, surface properties, and pore size distribution, on amine functionalization, thereby establishing critical structure–property relationships for kaolinite-based adsorbents. The successful implementation of this research provides theoretical guidance for large-scale CO_2 capture applications, fosters interdisciplinary integration between mineral processing, materials science, and chemistry, expands the utilization of natural clay mineral resources, and advances the development of high-performance mineral-based functional composite materials.

2. Experimental Section

2.1. Materials

Pristine kaolins (kaolinite and halloysite) with different morphologies, i.e., flake-like kaolinite (FK), tubular halloysite (TK) and rod-like kaolinite (RK), used were obtained from Suzhou, Fujian and Guangdong, China, respectively. Polyethyleneimine (branched PEI, MW ≈ 600) and 3-aminopropyltriethoxysilane (APTES, $C_9H_{23}NO_3Si$, molecular weight 221.37) were purchased from Aladdin Chemical Co., Ltd., Shanghai, China. All reagents are analytical grade and can be used without further purification.

2.2. Adsorbent Preparation

As shown in Figure 1, pristine kaolins were firstly calcined at 900 °C for 4 h (ramp rate: 5 °C/min) in air to optimize the pore size, increase surface activity and remove impurities [34,35]. In total, 10 g of calcined kaolins were added into 300 mL of 6 mol/L hydrochloric acid solution. The mixture was sealed and magnetically stirred at 80 °C for 6 h. The suspension was then filtered, water-washed and dried at 110 °C for 12 h to produce acid-activated kaolins (AFTRK, i.e., AFK, ATK and ARK).

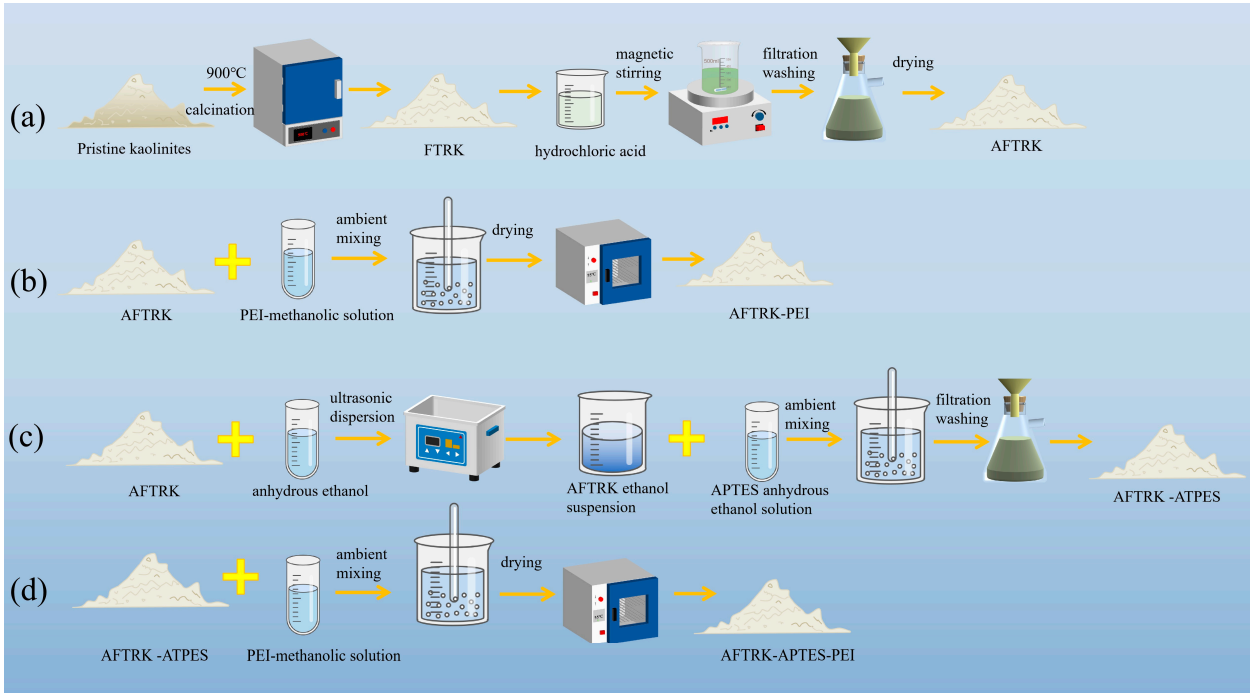


Figure 1. Schematic illustration for as-synthesized adsorbents and structural evolution process: (**a**) Pretreatment of kaolins with different morphologies; Preparation of different adsorbents: (**b**) AFTRK-PEI, (**c**) AFTRK-ATPES, (**d**) AFTRK-ATPES-PEI.

In total, 0.5 g AFTRK and 0.25 mL APTES were, respectively, dispersed in equal amounts of anhydrous ethanol solution and then mixed to form a homogeneous suspension. The mixtures were stirred at room temperature for 24 h, filtered, washed thoroughly with anhydrous ethanol, and dried at 80 °C for 12 h to obtain the APTES-grafted acid-activated kaolins (AFTRK-APTES adsorbents, i.e., AFK-APTES, ATK-APTES, ARK-APTES).

In total, 0.3 g AFTRK or 0.3 g AFTRK-APTES was added into the PEI methanolic solution, respectively. The mixtures were stirred at room temperature for 24 h and dried at 55 °C to yield PEI-impregnated acid-activated kaolins (AFTRK-PEI adsorbents, i.e., AFK-PEI, ATK-PEI, ARK-PEI) and hybrid amine-modified samples (AFTRK-APTES-PEI adsorbents).

2.3. Sample Characterization

Powder X-ray diffraction (XRD, Rigaku, D/MAX2550VB+, Tokyo, Japan) measurements of the samples were recorded on an X-ray diffractometer using Cu Kα radiation (λ = 0.15406 nm) at a scanning rate of 0.02°/s with a voltage of 40 kV and 40 mA. Fourier transform infrared (FT-IR, Thermo Nicolet Corporation, Nicolet Nexus 670, Waltham, MA, USA) spectra of the samples over the range of 4000~400 cm^{-1} were recorded on an FT-IR spectrophotometer using KBr pellets, and the mixture was pressed into a pellet for IR measurement. Morphological analysis was performed using a scanning electron microscope (SEM; Hitachi S-4800, Tokyo, Japan) and transmission electron microscopy (TEM, JEOL JEM-2100F, Tokyo, Japan). For sample preparation, the powdered specimens were uniformly dispersed on a conductive carbon tape-mounted stub, followed by sputter-coating with a thin layer of gold (5–10 nm) to enhance conductivity prior to SEM observation. The as-synthesized samples for TEM analysis were dispersed in ethanol by ultrasound and a drop of each solution was deposited on a Cu grid coated by a holed carbon film and dried in air. The N_2 adsorption–desorption measurements were performed on an ASAP 2020 PLUS HD88 Surface Area analyzer (Micromeritics, Atlanta, GA, USA) to view the pore structures of samples. These data were converted to specific surface area (S_{BET}) and total pore volume (V_{pores}) of these samples via the Brunauer–Emmett–Teller equation.

2.4. CO_2 Sorption/Desorption Performances

The CO_2 adsorption–desorption performances were recorded under atmospheric pressure using thermogravimetric analysis coupled with mass spectrometry (TGA-MS, SDT650, TA instruments, New Castle, DE, USA). Prior to testing, all samples were pretreated by degassing at 100 °C for 60 min under a pure nitrogen flow (40 mL/min) to eliminate residual moisture, solvents, and pre-adsorbed CO_2. Adsorption experiments were conducted in a mixed gas stream containing 40 mL/min N_2 and 60 mL/min CO_2 at 75 °C for 60 min. Subsequently, the gas flow was switched to pure N_2 (40 mL/min), and the temperature was ramped to 110 °C at a heating rate of 10 °C/min. The desorption phase was maintained at 110 °C for 40 min to ensure complete CO_2 release. The CO_2 adsorption capacity (mmol/g) was determined by the mass gain during the adsorption phase relative to the degassed sample baseline. Ten consecutive adsorption–desorption cycles were performed to evaluate the reproducibility and stability of different adsorbents.

3. Results and Discussion

Figure 2 exhibits the XRD patterns, FT-IR spectra and textural characteristics of different samples. As shown in Figure 2a, the raw tubular sample TK phase is halloysite with a specific diffraction peak and ordered crystal structure. The ATK modified by acid leaching is transformed into amorphous silica [24]. After APTES grafting modification, PEI impregnation modification and impregnation–grafting combined modification, the characteristic diffraction peaks of ATK did not change significantly. However, the char-

acteristic diffraction peak intensity of ATK-APTES-PEI was reduced and increased the amorphous proportion of the material. This phenomenon is likely attributed to the introduction of amorphous or low-crystallinity organic components through the chemical grafting of APTES and physical impregnation of PEI, which subsequently covered or filled the pores and surfaces of the carrier.

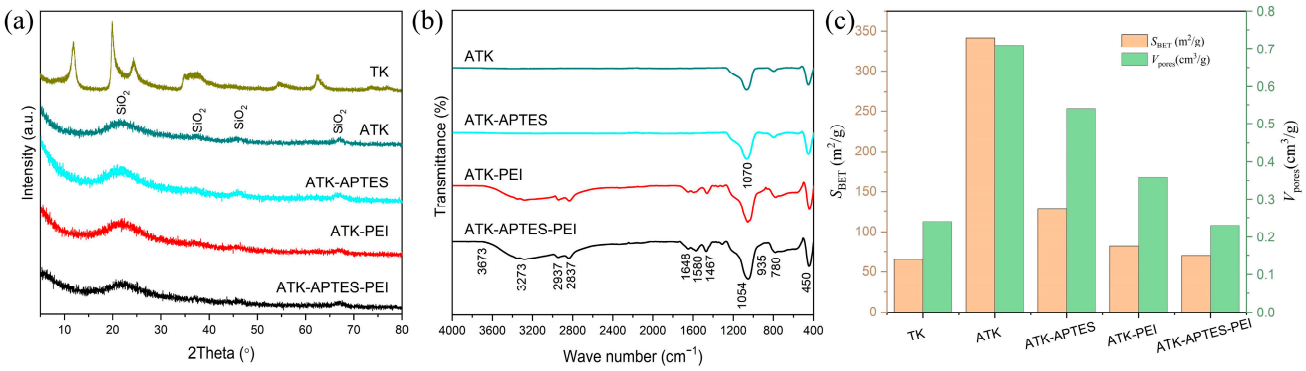


Figure 2. (**a**) XRD patterns, (**b**) FT-IR spectra of different adsorbents, (**c**) specific surface area and pore volume of tubular samples.

As shown in Figure 2b, during APTES grafting modification, the $-NH_2$ group in APTES reacts with the $-OH$ group on the surface of ATK. After PEI impregnation modification, the absorption peak at 3273 cm^{-1} is attributed to the vibration of the internal hydroxyl group. The bending vibration peaks of $-NH_2$ appear at 1580 and 1467 cm^{-1}, and the tensile vibration peaks of $-CH_2$ appear at 2837 and 2937 cm^{-1}, indicating that PEI is successfully loaded in the channel and pore structure of ATK. However, the symmetric bending vibration of ATK-APTES at 1470 cm^{-1} ascribed to the protonated amino group ($-NH_3^+$) [36], confirming the successful grafting of APTES on the surface of ATK, did not exhibit pronounced peak intensity, likely due to the low APTES grafting density or limited FT-IR detection sensitivity, where the characteristic $-NH_3^+$ signal might be obscured by background noise. After impregnation–grafting combined modification, the absorption peaks at 1580 and 1467 cm^{-1}, 2837 and 2937 cm^{-1}, 3273 cm^{-1} are assigned to the bending vibrations of $-NH_2$, the tensile vibrations of $-CH_2$ and the vibration of internal hydroxyl groups, respectively [37]. The intensity of the absorption peaks from 1470 to 3673 cm^{-1} attributed to the coordination and adsorbed water decreased significantly, indicating that $-NH_2$ groups in APTES reacted with $-OH$ on the surface of ATK-PEI. Therefore, after impregnation–grafting combined modification, a part of $-NH_2$ is successfully grafted on the surface of ATK, and the other part of $-NH_2$ is loaded in the pores of ATK. This amine-functionalization method is beneficial to improve the efficiency of amino group loading and thereby improve the CO_2 adsorption capacity and cyclic stability of the adsorbents.

Figure 2c presents the specific surface area and pore volume data of tubular samples subjected to different treatments. TK exhibited a relatively low specific surface area and pore volume. Acid treatment increases both parameters for ATK by removing impurities and enlarging pores. ATK-APTES showed a slight reduction in specific surface area and pore volume, likely attributed to the occupation of pore spaces by APTES molecules. PEI-impregnated ATK-PEI has lower values than ATK, as PEI fills the pores and the inside of the tube. ATK-APTES-PEI displayed the lowest values, suggesting synergistic pore filling by both APTES and PEI, which optimized the pore structure. Notably, despite the reduced porosity, the chemically introduced active sites and enhanced alkaline environment significantly improved CO_2 adsorption performance.

Figure 3 exhibits the morphology and microstructure of different adsorbents. As illustrated, after the acid leaching treatment, the tubular microstructure of the pristine halloysite did not undergo significant changes (Figure 3a,c). Under the action of hydrogen ions, the aluminum–oxygen octahedra on the inner wall of halloysite dissolved, releasing Al^{3+} and increasing the inner diameter, transforming it into tubular silica with a rough inner surface and higher porosity. This structure provides a large encapsulation capacity and excellent absorption performance. After organic amine grafting and impregnation, ATK-APTES-PEI exhibits noticeable aggregation, with gel-like PEI chains adsorbed on the surface of ATK and filling the pore structures. Meanwhile, some residual micropores remained inside the ATK tubes (Figure 3b,d). The formation of these interconnected pores provides channels for the rapid diffusion and mass transfer of CO_2 gas, effectively overcoming diffusion resistance within the adsorbent and thereby enhancing CO_2 adsorption performance.

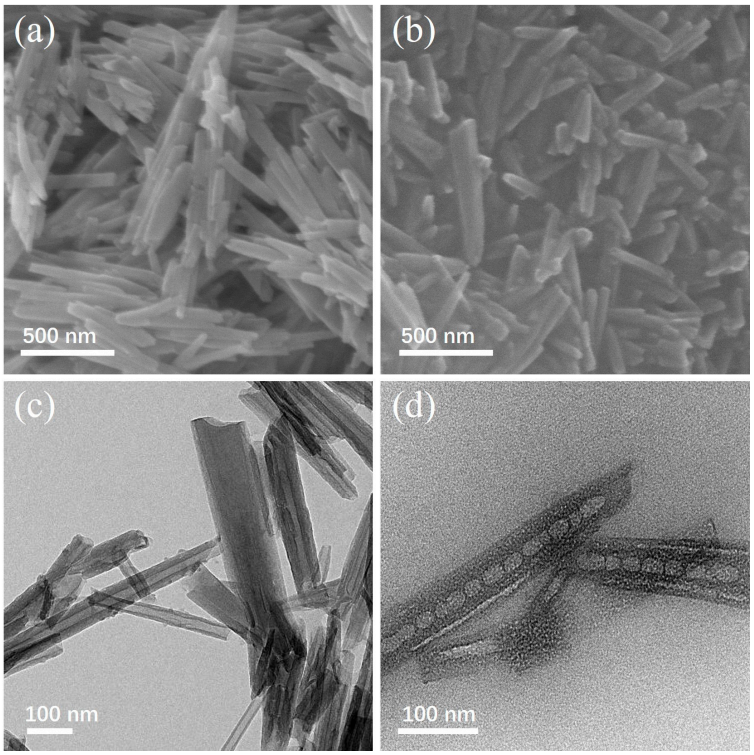


Figure 3. SEM and TEM images of different adsorbents: (**a**,**c**) ATK, (**b**,**d**) ATK-APTES-PEI.

Figure 4a presents the adsorption–desorption performance of the ATK-APTES-PEI sample. Under a 40% N_2/60% CO_2 atmosphere, the sample weight increases over time as CO_2 adsorbs onto the sample surface. The initial rapid weight gain arises from CO_2 adsorbing quickly at the active sites. As the curve flattens, adsorption nears saturation, and the rate slows due to occupied active sites. Upon switching to 100% N_2 and heating to 110 °C, the sample weight drops sharply as CO_2 desorbs rapidly, freeing the active sites and enabling sample regeneration. These results demonstrate that the hybrid amine-modified ATK-APTES-PEI sample maintained robust cyclic stability and regeneration capability throughout the adsorption–desorption process.

The CO_2 adsorption performance of the as-synthesized adsorbents was evaluated. By analyzing the CO_2 adsorption curves at 75 °C, the influence of amino-functionalization methods on the CO_2 adsorption performance of the adsorbents was systematically investigated. As shown in Figure 4b, the CO_2 adsorption capacity of unfunctionalized ATK is weak. After grafting with APTES, the CO_2 adsorption capacity of ATK-APTES reaches 0.55 mmol/g. After impregnation with PEI, the CO_2 adsorption capacity of ATK-PEI

reaches 1.11 mmol/g. The addition of APTES and PEI increases the surface active sites and alkalinity of the sample, thereby enhancing CO_2 adsorption. After grafting with APTES and impregnation with PEI, the CO_2 adsorption capacity of ATK-APTES-PEI reaches 1.68 mmol/g. Hybrid amine modification (combining grafted and impregnated amines) significantly enhances CO_2 adsorption capacity compared to single amine functionalization (either grafting or impregnation alone). The superior performance of the hybrid amine system can be attributed to the synergistic effect of chemically bonded and physically adsorbed amine species, which not only improve CO_2 uptake but also enhance cyclic stability during adsorption–desorption processes.

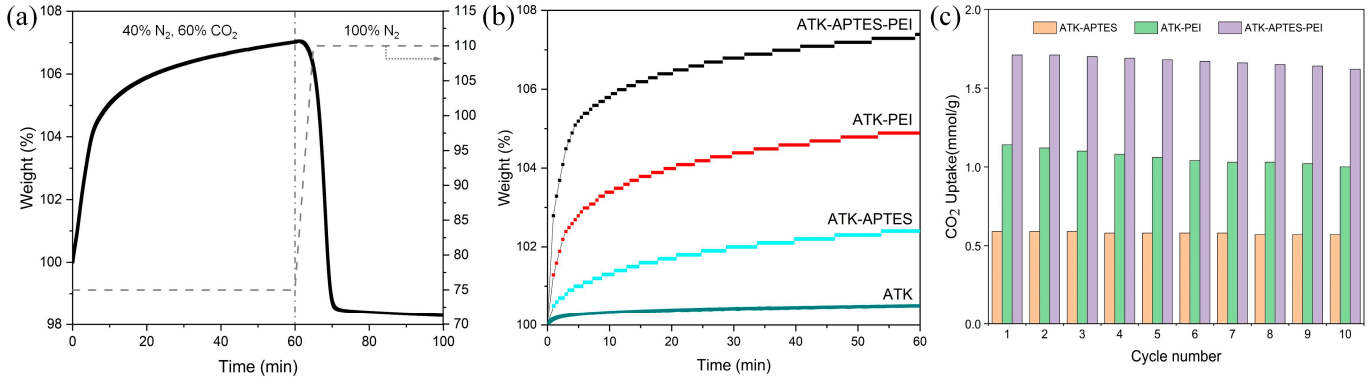


Figure 4. (**a**) Performance curve of one adsorption–desorption cycle of ATK-APTES-PEI; (**b**) CO_2 adsorption performance curves; (**c**) cyclic stability of different adsorbents.

Figure 4c shows the cyclic stability for different adsorbents. Under the testing conditions (adsorption at 75 °C for 2 h in a flow of 40 mL/min N_2 and 60 mL/min CO_2; desorption at 110 °C for 40 min in the flow of 40 mL/min pure N_2), ATK-APTES-PEI exhibited only a 5.3% decrease in CO_2 adsorption capacity after 10 adsorption–desorption cycles. Under the same conditions, ATK-APTES and ATK-PEI showed capacity reductions of 3.5% and 12.4%, respectively. These results demonstrate that while chemically grafted amines do not significantly enhance CO_2 adsorption capacity, they markedly improve cycling stability. In contrast, physical impregnated amines (PEIs) effectively increase adsorption capacity but offer limited stability enhancement. Therefore, the combined use of grafted and impregnated amines achieves a synergistic improvement in both adsorption capacity and cyclic stability of the adsorbents.

Figure 5 presents the XRD patterns of amine-functionalized kaolinite-based CO_2 solid adsorbents with different morphologies, characterizing and comparatively analyzing their crystal structures. The experimental results demonstrate that after calcination activation and acid leaching treatment, all three morphologies of kaolinite transformed from their original kaolinite structure to silica structures. Notably, the ARK and AFK contained both amorphous silica and crystalline silica phases, as evidenced by the sharp diffraction peaks appearing at $2\theta = 21°$ and 27°. In contrast, ATK completely transformed into amorphous silica. Furthermore, the ATK exhibited a larger specific surface area, abundant pore structures, and superior surface characteristics. These advantageous properties endow ATK and its modified adsorbents with greater potential for CO_2 adsorption compared to other morphologies.

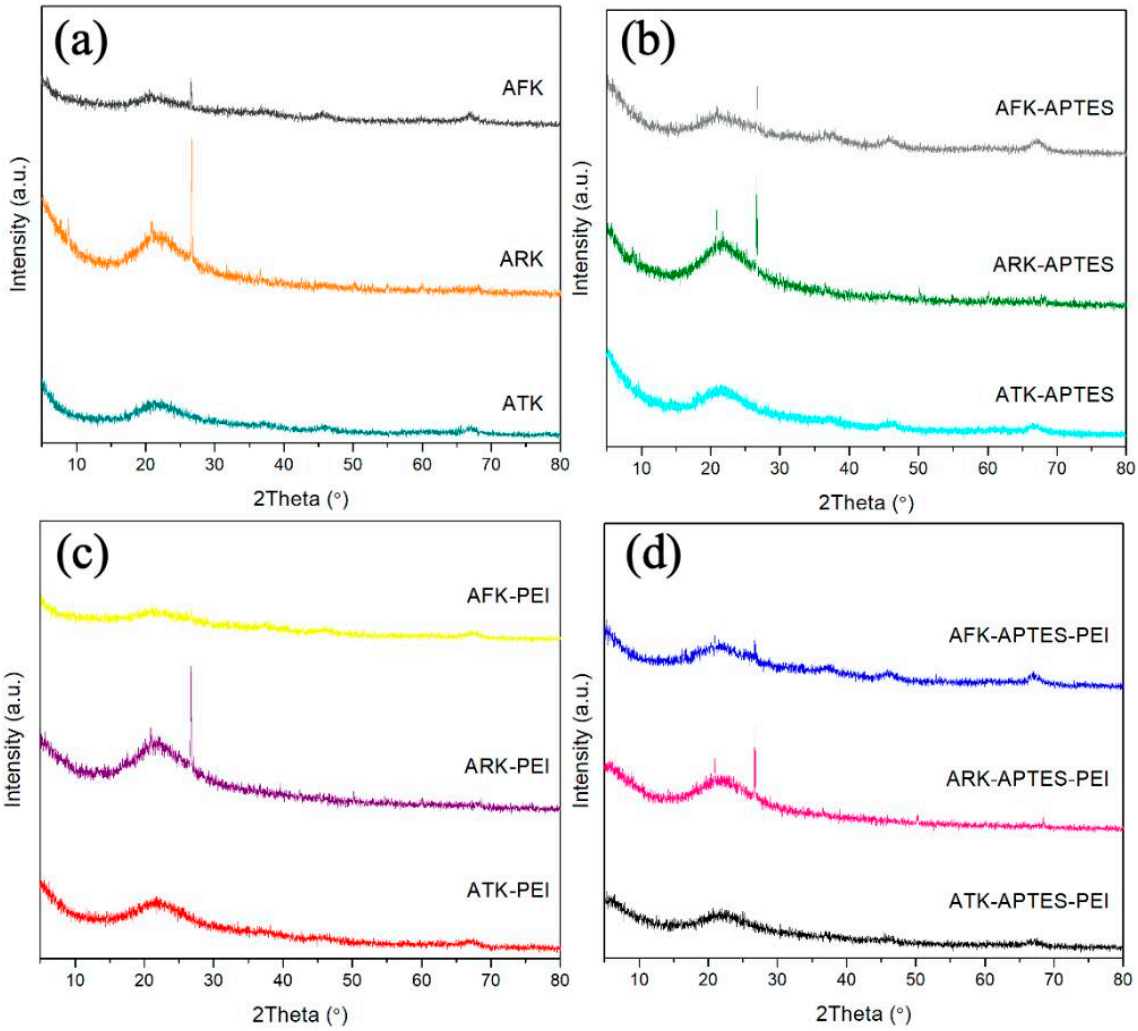


Figure 5. XRD patterns of amine-functionalized kaolinite-based CO_2 solid adsorbents with different morphologies: (**a**) acid treatment samples; (**b**) APTES grafting-modified samples; (**c**) PEI impregnation-modified samples; (**d**) hybrid impregnation–grafting-modified samples.

As shown in Figure 6, the FT-IR spectra of amine-functionalized kaolinite-based CO_2 solid adsorbents with different morphologies indicated the successful amine functionalization ($-NH_2$ loading) of acid-leached kaolinite samples through both APTES grafting and PEI impregnation. The APTES grafting-modified samples with different morphologies showed similar FT-IR peak intensities for characteristic chemical groups. This indicates comparable surface properties across different morphologies after acid treatment. However, among the PEI impregnation-modified samples, ATK-PEI exhibited stronger vibration peaks for $-NH_2$ and $-CH_2$ groups, indicating enhanced organic amine loading capacity in tubular structures. Meanwhile, the robust interfacial adhesion in tubular samples contributes to the improved CO_2 adsorption performances. The comparative analysis reveals that while all morphologies achieved successful functionalization, the tubular architecture provides distinct advantages for amine loading and subsequent CO_2 capture applications.

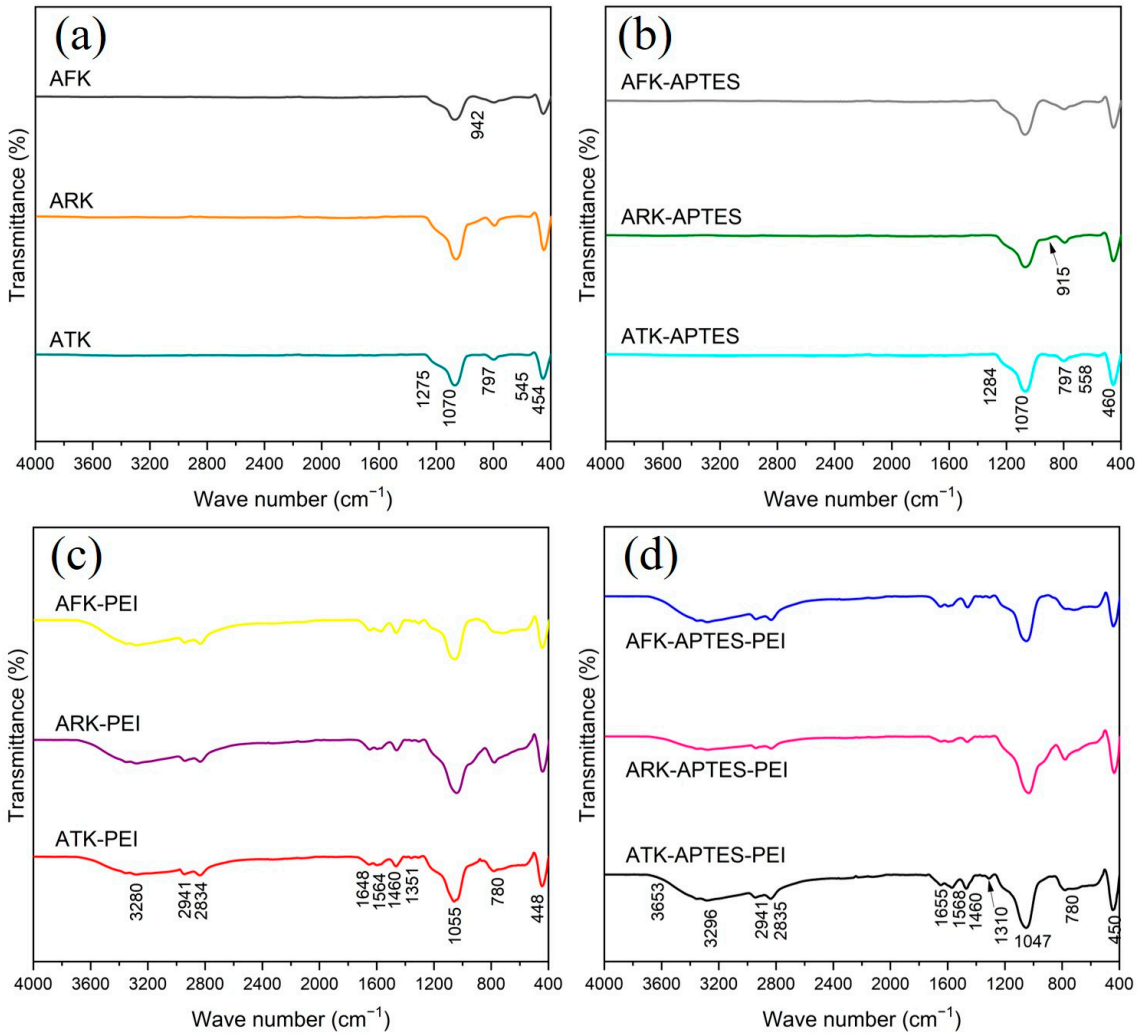


Figure 6. FT-IR spectra of amine-functionalized kaolinite-based CO_2 solid adsorbents with different morphologies: (**a**) acid treatment samples; (**b**) APTES grafting-modified samples; (**c**) PEI impregnation-modified samples; (**d**) hybrid impregnation–grafting-modified samples.

Figure 7 presents the micromorphology of amine-functionalized kaolinite-based CO_2 solid adsorbents with different morphologies, clearly revealing the natural flake-like, tubular and rod-like configurations of the pristine kaolinite supports. Following acid treatment, which effectively removed surface impurities and dissolved Al^{3+} from the mineral network to convert kaolinite into amorphous silica [38], the three morphologies exhibited markedly different responses to subsequent amine functionalization (via grafting, impregnation, or hybrid amine modification). The flake-like samples suffered from severe particle aggregation with insufficient pore channels for effective amine loading, while the rod-like samples, though capable of forming packed pore structures, showed complete pore filling by organic amines that eliminated residual pores for CO_2 diffusion. In striking contrast, the tubular samples uniquely preserved both its stacking pores and intrinsic tubular channels after functionalization, creating an optimal hierarchical porous structure that simultaneously enhanced amine loading capacity and maintained unimpeded CO_2 transport pathways, thereby establishing an ideal structural foundation for superior CO_2 adsorption performance through this multiscale porous network.

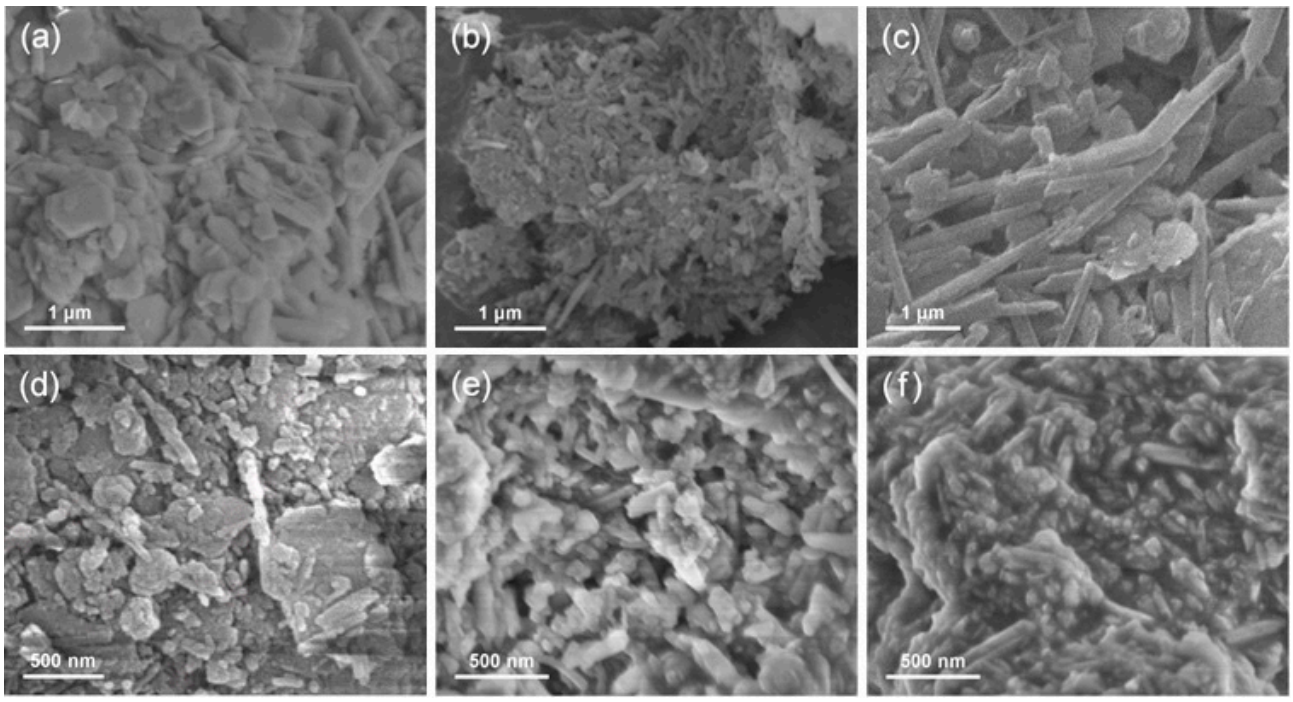


Figure 7. SEM images of amine-functionalized kaolinite-based CO_2 solid adsorbents with different morphologies: (**a**) AFK; (**b**) ATK; (**c**) ARK; (**d**) AFK-APTES-PEI; (**e**) ATK-APTES-PEI; (**f**) ARK-APTES-PEI.

The CO_2 adsorption performances of the as-synthesized adsorbents were systematically evaluated through TGA measurements under set conditions (adsorption at 75 °C for 2 h in a flow of 40 mL/min N_2 and 60 mL/min CO_2; desorption at 110 °C for 40 min in the flow of 40 mL/min pure N_2), with a particular focus on how amine functionalization and morphological variations in kaolinite-based adsorbents influenced CO_2 adsorption behavior. As illustrated in Figure 8a, APTES-grafted samples exhibited generally weak adsorption capacity, with AFK-APTES and ARK-APTES showing negligible weight gains (<1%) during testing, while ATK-APTES demonstrated superior performance with a 2.4% weight gain, highlighting the advantage of tubular morphology. PEI-impregnated samples displayed moderate adsorption capacity overall, where AFK-PEI (3.3% weight gain) slightly outperformed ATK-APTES but remained inferior to both ARK-PEI and ATK-PEI, the latter achieving the highest individual capacity at 4.9% weight gain among single functionalization samples. Notably, the hybrid amine-functionalized samples universally surpassed their single functionalization counterparts. While AFK-APTES-PEI showed only marginal improvement over ATK-PEI (5.4% vs. 4.9%), the tubular ATK-APTES-PEI achieved a remarkable 7.4% weight gain, ultimately delivering the highest recorded capacity of 1.68 mmol/g. These results clearly demonstrate that both the amine loading strategy and support morphology critically determine adsorption performances: (i) dual functionalization yields optimal results, and (ii) tubular architecture provides superior structural advantages. The exceptional performance of ATK-APTES-PEI establishes it as the premier adsorbent configuration, combining the benefits of tubular morphology's enhanced surface accessibility with the synergistic effects of hybrid amine functionalization.

The CO_2 absorption capacities of amine-impregnated, APTES-grafted, and mixed amine-loaded adsorbents on porous materials under various conditions are summarized in Table 1. The ATK-APTES-PEI adsorbent developed in this work achieved an excellent balance between CO_2 adsorption capacity (1.68 mmol/g) and cyclic stability (5.3% capacity loss) through hierarchical pore structure design and a mixed amine strategy while significantly reducing costs by utilizing natural clay as the raw material. Compared to

the materials listed in Table 1, its advantages lie in the following: (i) its adsorption capacity approaching that of high-cost materials (e.g., SBA-15), (ii) its stability surpassing most mineral-based adsorbents, (iii) its simplified synthesis steps eliminating the need for expensive reagents, and (iv) its suitability for industrial applications.

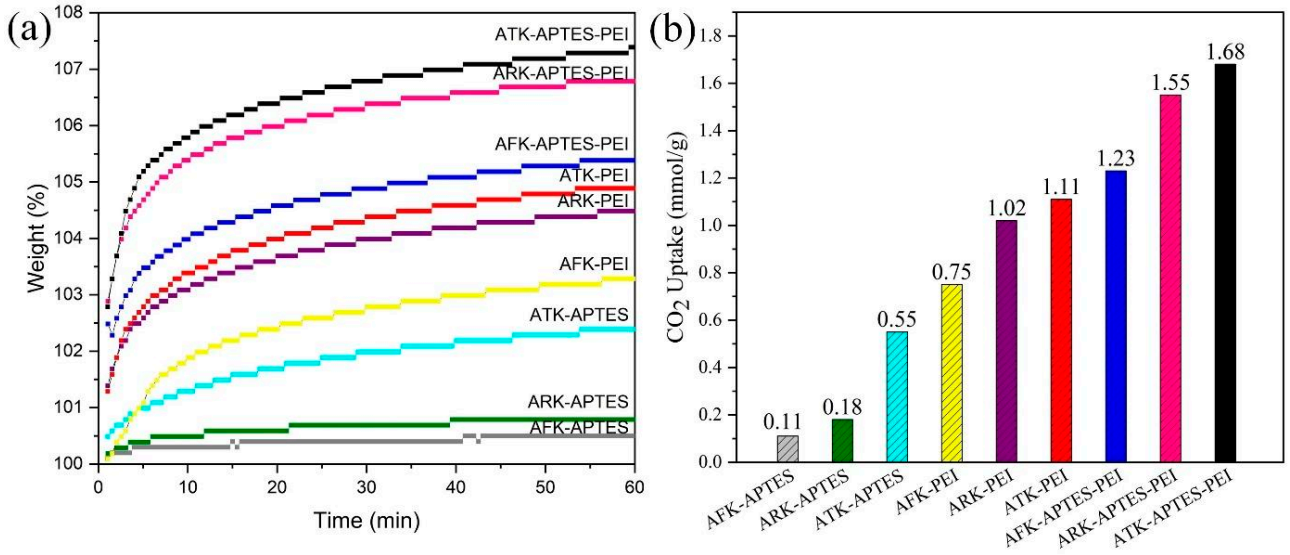


Figure 8. (**a**) CO_2 adsorption performance curves at 75 °C for 2 h in a flow of N_2/CO_2; (**b**) comparison of CO_2 uptake capacity of different adsorbents.

Table 1. CO_2 adsorption performances of solid amine adsorbents with various porous supports and different amines.

Supports	Amine Type	Amine Loading (wt.%)	Adsorption Conditions		CO_2 Uptake (mmol/g)	Ref.
			T (°C)	Atmosphere		
ATK	APTES	32.11	75	60%CO_2/40%N_2	0.55	This study
ATK	PEI	40	75	60%CO_2/40%N_2	1.11	This study
ATK	APTES-PEI	60	75	60%CO_2/40%N_2	1.68	This study
AFK	APTES-PEI	60	75	60%CO_2/40%N_2	1.23	This study
ARK	APTES-PEI	60	75	60%CO_2/40%N_2	1.55	This study
Zeolite Beta	Alkyl-APTES	-	90	15%CO_2/85%N_2	1.44	[39]
Industrial Waste Silica Fume	TEPA	30	50	99.999% CO_2	2.22	[40]
MSU-1 Halloysite	APTES	48	25	100% air	0.13	[27]
Halloysites	PEI	20	80	60%CO_2/40%N_2	0.87	[41]
Halloysites	AP-PEI	20/40	80	50%CO_2/50%N_2	1.51	[42]
SBA-15	APTS	15	25	10%CO_2	2.01	[43]

4. Conclusions

This study developed an innovative approach for synthesizing high-performance CO_2 adsorbents through acid leaching and the subsequent grafting–impregnation amine-functionalization of polymorphic kaolinite minerals. The preparation methodology profoundly alters the structural and chemical characteristics of kaolinite substrates, inducing significant phase transformations and pore structure modifications that enhance adsorption performance, thereby establishing a novel functionalization technique for morphologically diverse kaolinite minerals. Tubular adsorbents exhibit superior performances compared to rod-like and flake-like counterparts due to their unique hierarchical porous structure formed through thermal treatment, acid leaching, and amine functionalization, which not only maximizes organic amine loading efficiency through increased substrate–amine interfacial contact but also maintains residual pores for efficient CO_2 diffusion and mass

transfer. The synergistic combination of grafted and impregnated amine groups simultaneously improves both adsorption capacity and cyclic stability, with the optimized tubular composite demonstrating exceptional CO_2 capture performances that show great promise for industrial-scale applications. These findings provide fundamental insights into the structure–property relationships of mineral-based adsorbents and offer practical guidance for designing high-efficiency CO_2 capture adsorbents.

Author Contributions: X.L.: project administration, writing—original draft, writing—review and editing; J.C.: writing—original draft, investigation, formal analysis, data curation; W.Z.: data curation, formal analysis; C.W.: data curation, formal analysis; H.M.: data curation, formal analysis; K.P.: supervision, project administration, methodology; Z.Z.: conceptualization, investigation. All authors have read and agreed to the published version of the manuscript.

Funding: This research was funded by the Research Funds for the Interdisciplinary Projects, CHU (300104240916), the Fundamental Research Funds for the Central Universities (300102314301), and the Key Research and Development Project of Shaanxi Province of China (2025GX-YBXM-352).

Data Availability Statement: All data generated or analyzed during this study are included in this published article.

Conflicts of Interest: Zheng Zhou is affiliated with the company State Grid Zhejiang Electric Power Research Institute. The remaining authors declare that the research was conducted in the absence of any commercial or financial relationships that could be construed as a potential conflict of interest.

Abbreviations

The following abbreviations are used in this manuscript:

CCS	Carbon capture and storage
MOFs	Metal–organic frameworks
FK	Flake-like kaolinite
TK	Tubular halloysite
RK	Rod-like kaolinite
APTES	3-aminopropyltriethoxysilane
AFTRK	Acid-activated kaolin
AFTRK-APTES	APTES-grafted acid activated kaolin
AFTRK-PEI	PEI-impregnated acid activated kaolin
AFTRK-APTES-PEI	Hybrid amine-modified sample
XRD	Powder X-ray diffraction
FT-IR	Fourier transform infrared
SEM	Scanning electron microscope
TEM	Transmission electron microscopy
TGA-MS	Thermogravimetric analysis coupled with mass spectrometry
SBA-15	Santa Barbara Amorphous-15

References

1. Armstrong, R.C.; Wolfram, C.; de Jong, K.P.; Gross, R.; Lewis, N.S.; Boardman, B.; Ragauskas, A.J.; Ehrhardt-Martinez, K.; Crabtree, G.; Ramana, M.V. The frontiers of energy. *Nat. Energy* **2016**, *1*, 15020. [CrossRef]
2. Li, X.; Li, R.; Peng, K.; Zhao, K.; Bai, M.; Li, H.; Gao, W.; Gong, Z. Amine-impregnated porous carbon–silica sheets derived from vermiculite with superior adsorption capability and cyclic stability for CO_2 capture. *Chem. Eng. J.* **2023**, *464*, 142662. [CrossRef]
3. Peng, K.; Ye, J.; Wang, H.; Song, H.; Deng, B.; Song, S.; Wang, Y.; Zuo, L.; Ye, J. Natural halloysite nanotubes supported Ru as highly active catalyst for photothermal catalytic CO_2 reduction. *Appl. Catal. B-Environ.* **2023**, *324*, 122262. [CrossRef]
4. Hunka, N.; Duncanson, L.; Armston, J.; Dubayah, R.; Healey, S.P.; Santoro, M.; May, P.; Araza, A.; Bourgoin, C.; Montesano, P.M.; et al. Intergovernmental Panel on Climate Change (IPCC) Tier 1 forest biomass estimates from Earth Observation. *Sci. Data* **2024**, *11*, 1127. [CrossRef]
5. Haszeldine, R.S. Carbon capture and storage: How green can black be? *Science* **2009**, *325*, 1647–1652. [CrossRef]

6. Shao, B.; Wang, Z.Q.; Gong, X.Q.; Liu, H.; Qian, F.; Hu, P.; Hu, J. Synergistic promotions between CO_2 capture and in-situ conversion on Ni-CaO composite catalyst. *Nat. Commun.* **2023**, *14*, 996. [CrossRef]
7. Wang, J.Y.; Huang, L.; Yang, R.Y.; Zhang, Z.; Wu, J.W.; Gao, Y.S.; Wang, Q.; O'Hare, D.; Zhong, Z.Y. Recent advances in solid sorbents for CO_2 capture and new development trends. *Energy Environ. Sci.* **2014**, *7*, 3478–3518. [CrossRef]
8. Creamer, A.E.; Gao, B. Carbon-based adsorbents for postcombustion CO_2 capture: A critical review. *Environ. Sci. Technol.* **2016**, *50*, 7276–7289. [CrossRef]
9. Loganathan, S.; Ghoshal, A.K. Amine tethered pore-expanded MCM-41: A promising adsorbent for CO_2 capture. *Chem. Eng. J.* **2017**, *308*, 827–839. [CrossRef]
10. Ahsan, S.; Ayub, A.; Meeroff, D.; Lashak, M.J. A comprehensive comparison of zeolite-5A molecular sieves and amine-grafted SBA-15 silica for cyclic adsorption-desorption of carbon dioxide in enclosed environments. *Chem. Eng. J.* **2022**, *437*, 135139. [CrossRef]
11. Li, X.; Zhao, X.; Meng, Y.; Xue, H.; Chen, J.; Peng, K. Additive promoted supported mixed amines on mesoporous silica for cyclic capture of carbon dioxide. *Sep. Purif. Technol.* **2025**, *362*, 131824. [CrossRef]
12. Kim, J.; Lin, L.-C.; Swisher, J.A.; Haranczyk, M.; Smit, B. Predicting large CO_2 adsorption in aluminosilicate zeolites for postcombustion carbon dioxide capture. *J. Am. Chem. Soc.* **2012**, *134*, 18881–19308. [CrossRef] [PubMed]
13. Shi, Y.Q.; Zhu, J.; Liu, X.Q.; Geng, J.C.; Sun, L.B. Molecular template-directed synthesis of microporous polymer networks for highly selective CO_2 capture. *ACS. Appl. Mater. Interfaces* **2014**, *6*, 20340–20349. [CrossRef] [PubMed]
14. Zhang, Z.J.; Yao, Z.Z.; Xiang, S.C.; Chen, B.L. Perspective of microporous metal-organic frameworks for CO_2 capture and separation. *Energy Environ. Sci.* **2014**, *7*, 2868–2899. [CrossRef]
15. McDonald, T.M.; Mason, J.A.; Kong, X.; Bloch, E.D.; Gygi, D.; Dani, A.; Crocellà, V.; Giordanino, F.; Odoh, S.O.; Drisdell, W.S.; et al. Cooperative insertion of CO_2 in diamine-appended metal-organic frameworks. *Nature* **2015**, *519*, 303–308. [CrossRef]
16. Qin, C.L.; Yin, J.J.; Ran, J.Y.; Zhang, L.; Feng, B. Effect of support material on the performance of K_2CO_3 based pellets for cyclic CO_2 capture. *Appl. Energy* **2014**, *136*, 280–288. [CrossRef]
17. Zhao, T.X.; Guo, B.; Zhang, F.; Sha, F.; Li, Q.; Zhang, J.B. Morphology control in the synthesis of $CaCO_3$ microspheres with a novel CO_2-storage material. *ACS Appl. Mater. Interfaces* **2015**, *7*, 15918–15927. [CrossRef]
18. Wang, W.L.; Xiao, J.; Wei, X.L.; Ding, J.; Wang, X.X.; Song, C.S. Development of a new clay supported polyethylenimine composite for CO_2 capture. *Appl. Energy* **2014**, *113*, 334–341. [CrossRef]
19. Irani, M.; Fan, M.H.; Ismail, H.; Tuwati, A.; Dutcher, B.; Russell, A.G. Modified nanosepiolite as an inexpensive support of tetraethylenepentamine for CO_2 sorption. *Nano Energy* **2015**, *11*, 235–246. [CrossRef]
20. Sánchez-Zambrano, K.S.; Lima Duarte, L.; Maia, D.A.S.; Vilarrasa-García, E.; Bastos-Neto, M.; Rodríguez-Castellón, E.; de Azevedo, D.C.S. CO_2 capture with mesoporous silicas modified with amines by double functionalization: Assessment of adsorption/desorption cycles. *Materials* **2018**, *11*, 887. [CrossRef]
21. Chen, Y.-H.; Lu, D.-L. CO_2 capture by kaolinite and its adsorption mechanism. *Appl. Clay Sci.* **2015**, *104*, 221–228. [CrossRef]
22. Wang, Y.; Ding, Z.; Cao, Z.; Han, F.; Wang, Y.; Cheng, H. Molecular simulation of CO_2 adsorption on kaolinite: Insights into geological storage of CO_2. *Appl. Clay Sci.* **2024**, *258*, 107495. [CrossRef]
23. Chen, Y.H.; Lu, D.L. Amine modification on kaolinites to enhance CO_2 adsorption. *J. Colloid Interfaces Sci.* **2014**, *436*, 47–51. [CrossRef]
24. Ran, Y.; Peng, K.; Li, Z.; Guo, X.; Chen, H.; Cai, S.; Su, L.; Niu, M.; Lu, D.; Wang, H. Amine-Functionalized SiC nanowires aerogel synchronizes high capacity and ultra-rapid kinetics for CO_2 capture. *Chem. Eng. J.* **2025**, *514*, 163149. [CrossRef]
25. Kole, K.; Das, S.; Samanta, A.; Jana, S. Parametric study and detailed kinetic understanding of CO_2 adsorption over high-surface-area flowery silica nanomaterials. *Ind. Eng. Chem. Res.* **2020**, *59*, 21393–21402. [CrossRef]
26. de Sousa, J.A.R.; Amâncio, R.; Morales-Ospino, R.; de Oliveira, J.L.B.; Cecilia, J.A.; Vilarrasa-García, E.; Bastos-Neto, M.; Rodríguez-Castellón, E.; de Azevedo, D.C.S. H_2S and H_2O combined effect on CO_2 capture by amino functionalized hollow microsphere silicas. *Ind. Eng. Chem. Res.* **2021**, *60*, 10139–10154. [CrossRef]
27. Jana, S.; Das, S.; Ghosh, C.; Maity, A.; Pradhan, M. Halloysite nanotubes capturing isotope selective atmospheric CO_2. *Sci. Rep.* **2015**, *5*, 8711. [CrossRef]
28. Ko, Y.G.; Lee, H.J.; Oh, H.C.; Choi, U.S. Amines immobilized double-walled silica nanotubes for CO_2 capture. *J. Hazard Mater.* **2013**, *250*, 53–60. [CrossRef]
29. Sim, K.; Lee, N.; Kim, J.; Cho, E.B.; Gunathilake, C.; Jaroniec, M. CO_2 adsorption on amine-functionalized periodic mesoporous benzenesilicas. *ACS. Appl. Mater. Interfaces* **2015**, *7*, 6792–6802. [CrossRef]
30. Chai, S.H.; Liu, Z.M.; Huang, K.; Tan, S.; Dai, S. Amine functionalization of microsized and nanosized mesoporous carbons for carbon dioxide capture. *Ind. Eng. Chem. Res.* **2016**, *55*, 7355–7361. [CrossRef]
31. Builes, S.; Vega, L.F. Effect of Immobilized Amines on the Sorption Properties of Solid Materials: Impregnation versus Grafting. *Langmuir* **2013**, *29*, 199–206. [CrossRef] [PubMed]

32. Cecilia, J.A.; Vilarrasa-García, E.; García-Sancho, C.; Saboya, R.M.A.; Azevedo, D.C.S.; Cavalcante, C.L.; Rodríguez-Castellón, E. Functionalization of hollow silica microspheres by impregnation or grafted of amine groups for the CO_2 capture. *Int. J. Greenh. Gas Control* **2016**, *52*, 344–356. [CrossRef]
33. Chouikhi, N.; Cecilia, J.A.; Vilarrasa-García, E.; Besghaier, S.; Chlendi, M.; Duro, F.I.F.; Castellon, E.R.; Bagane, M. CO_2 adsorption of materials synthesized from clay minerals: A review. *Minerals* **2019**, *9*, 514. [CrossRef]
34. Xue, H.; Dong, X.; Fan, Y.; Ma, X.; Yao, S. Study of structural transformation and chemical reactivity of kaolinite-based high ash slime during calcination. *Minerals* **2023**, *13*, 466. [CrossRef]
35. Sánchez-Soto, P.J.; García-Garzón, V.; Martínez-Martínez, S.; Pérez-Villarejo, L.; Sánchez-Garrido, J.A.; Garzón, E. Influence of features and firing temperature on the ceramic properties and phase evolution of raw kaolins. *Constr. Build. Mater.* **2025**, *466*, 140215. [CrossRef]
36. Swasy, M.I.; Campbell, M.L.; Brummel, B.R.; Guerra, F.D.; Attia, M.F.; Smith, G.D.; Alexis, F.; Whitehead, D.C. Poly(amine) modified kaolinite clay for VOC capture. *Chemosphere* **2018**, *213*, 19–24. [CrossRef]
37. Li, X.; Li, H.; Zhao, X.; Zhao, Y.; Zhang, B.; Zhao, K.; Peng, K. Synergy tetraethylenepentamine and diethanolamine impregnated within silica nanotubes derived from natural halloysite for efficient CO_2 capture. *J. Clean. Prod.* **2024**, *434*, 140405. [CrossRef]
38. Du, C.; Yang, H. Investigation of the physicochemical aspects from natural kaolin to Al-MCM-41 mesoporous materials. *J. Colloid Interfaces Sci.* **2012**, *369*, 216–222. [CrossRef]
39. Liu, L.; Jin, S.; Ko, K.; Kim, H.; Ahn, I.S.; Lee, C.H. Alkyl-functionalization of (3-Aminopropyl) triethoxysilane-grafted zeolite beta for carbon dioxide capture in temperature swing adsorption. *Chem. Eng. J.* **2020**, *382*, 122834. [CrossRef]
40. Yang, F.; Xing, L.A.; Opoku, K.N.; Zhao, H.Y.; Wang, Z.X.; Ni, R.T.; Gao, Q.; Guo, Z.J.; Zeng, F.; Yuan, A.H.; et al. Wastes against wastes treatment: Industrial silica fume derived porous solid amine adsorbent for efficient and reversible ultralow-pressure CO_2 adsorption. *Sep. Purif. Technol.* **2025**, *352*, 128257. [CrossRef]
41. Li, X.Y.; Li, H.R.; Zhao, X.Q.; Peng, K. Amine-impregnated natural inorganic nanotubes via layer-by-layer electrostatically self-assembly approach for efficient CO_2 adsorption. *Sep. Purif. Technol.* **2024**, *349*, 127864. [CrossRef]
42. Wang, Z.L.; Pang, Y.H.; Guo, H.X.; Wang, H.; Liu, L.; Wang, X.; Zhang, S.; Cui, W.Q. Increased CO_2 capture capacity via amino-bifunctionalized halloysite nanotubes adsorbents. *Fuel* **2024**, *364*, 131036. [CrossRef]
43. Gray, M.L.; Soong, Y.; Champagne, K.J.; Pennline, H.W.; Baltrus, J.P.; Stevens, R.W.; Khatri, R.; Chuang, S.S.C.; Filburn, T. Improved immobilized carbon dioxide capture sorbents. *Abstr. Pap. Am. Chem. Soc.* **2004**, *86*, 1449–1455. [CrossRef]

Disclaimer/Publisher's Note: The statements, opinions and data contained in all publications are solely those of the individual author(s) and contributor(s) and not of MDPI and/or the editor(s). MDPI and/or the editor(s) disclaim responsibility for any injury to people or property resulting from any ideas, methods, instructions or products referred to in the content.